microPublication BIOLOGY

5/8/2025 - *Open Access*

Insertion of mNeonGreen into the variable domain of DRP-1 permits visualization of functional endogenous protein

Eric J. Lambie[1], Barbara Conradt[1§]

[1]Cell and Developmental Biology, University College London, London, England, United Kingdom

[§]To whom correspondence should be addressed: b.conradt@ucl.ac.uk

Abstract

We used CRISPR-Cas9 editing of the genomic *drp-1* locus in *C. elegans* to test whether the mitochondrial fission function of DRP-1 was retained following insertion of mNeonGreen into the variable domain. We found that DRP-1 activity remains largely intact despite this large internal insertion. Furthermore, in living cells, the internally tagged protein is readily detectable as discrete puncta associated with mitochondria, which presumably represent prospective mitochondrial scission sites. The internally tagged DRP-1 protein represents a powerful new tool for real time *in vivo* analyses of mitochondrial fission and DRP-1 function.

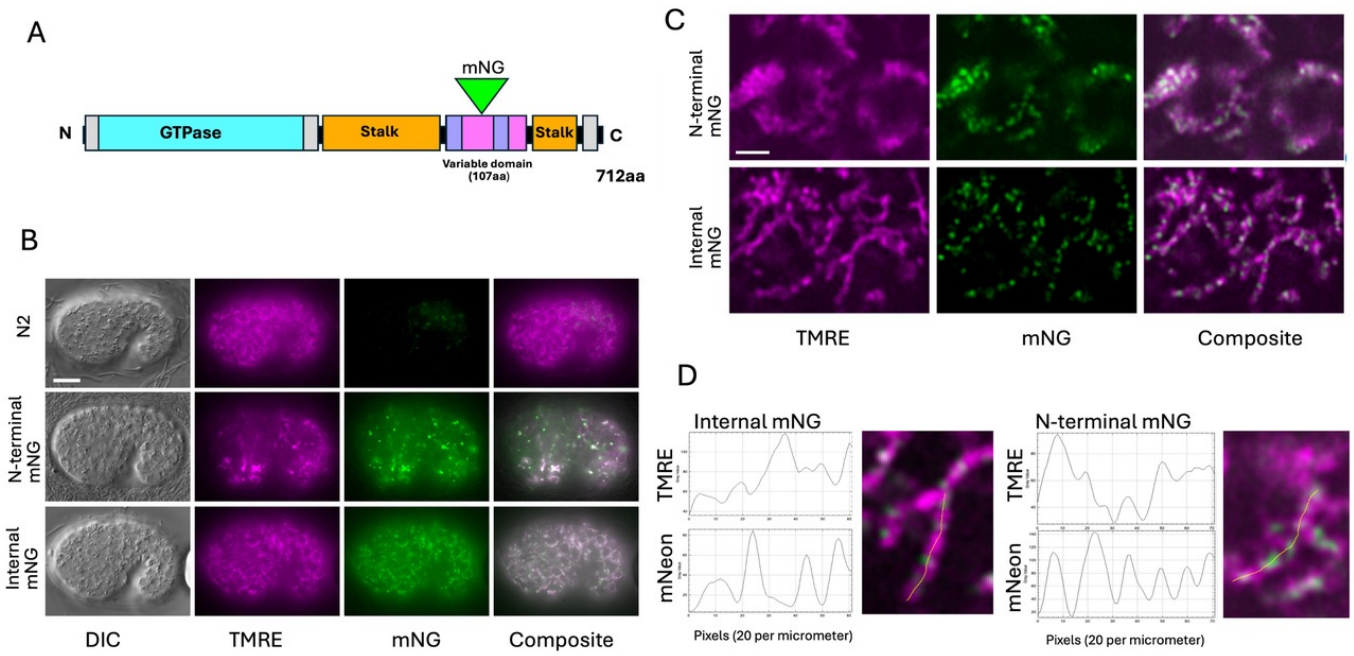

Figure 1. Internal tagging with mNeonGreen of *C. elegans* DRP-1 protein:

A. Cartoon representation of DRP-1b isoform showing site of mNG insertion into the variable domain. Gray boxes, BSE elements, lavender boxes, MorF1 and MorF2. In all panels, Internal mNG denotes *drp-1(dx230Internal)* and N-terminal mNG, *drp-1(dx224N-terminal).*

B. Widefield images of TMRE-stained comma stage embryos. Scale bar is 10 micrometers.

C. Super-resolution images of TMRE-stained embryos. Scale bar is 2 micrometers.

D. Line traces of TMRE and mNG intensity along representative mitochondria from panel C.

Description

DRP-1 is an evolutionarily conserved, ~80 kDa eukaryotic dynamin-like GTPase that mediates mitochondrial fission (Labrousse et al. 1999; Smirnova et al. 2001; Bleazard et al. 1999; Tábara, Segawa, and Prudent 2025; Kamerkar, Liu, and Higgs 2025). This function depends on the ability of DRP-1 to associate with the mitochondrial outer surface and assemble into helical multimers that cause mitochondrial constriction (Kalia et al. 2018; Rochon et al. 2024). Ultimately, this leads to mitochondrial scission, although the precise role of DRP-1 in the late events of this process is still under investigation (see Roy and Pucadyil 2022; Pérez-Jover et al. 2022). Visualization of functional DRP-1 *in vivo* is confounded by the fact that addition of protein tags to either the N- or C-terminus impairs DRP-1 function (Montecinos-Franjola et al. 2020). We used CRISPR-Cas9-mediated genome editing to test whether insertion of the mNeonGreen (mNG) fluorescent protein into the variable region (Figure 1 A) is compatible with DRP-1 function. The variable domain is not essential for the assembly of DRP multimers, but it is important for regulation of GTPase activity and proper binding to the outer mitochondrial membrane (Strack and Cribbs 2012; Liu and Chan 2015; Bui et al. 2012). We selected an insertion site that is situated between the conserved MoRF-1 helical region and the cardiolipin-binding domain (Mahajan et al. 2021). This position could potentially allow mNG to fit inside the DRP-1 multimeric complex assembled on the mitochondrial surface. Note that *C. elegans* *drp-1* gives rise to two isoforms, DRP-1a and DRP-1b (Sternberg et al. 2024). The b isoform contains 7 additional amino acids (VSAHGEQ) within the variable domain, and these are situated 4aa before the mNG insertion site (see Table 1). Therefore, both isoforms will be tagged with mNG. As a control, we also tested insertion of mNG at the N-terminus of DRP-1, as this is predicted to cause a loss-of-function phenotype (Montecinos-Franjola et al. 2020). We found that insertion of mNG at the N-terminus (*drp-1(dx224Nterm)*) resulted in 39% embryonic lethality (n = 1753). By contrast, insertion of mNG within the variable region (*drp-1(dx230Internal)*) resulted in only 9% embryonic lethality (n = 1994). Embryonic lethality in the wild type N2 control strain was 0.35% (n=1409). Neither fusion protein acts as a strong dominant negative, since embryonic lethality was very infrequent among the progeny of heterozygous mothers: Only 0.6 % of the progeny of *drp-1(dx230Internal)*/+ mothers failed to hatch (n = 476) and for *drp-1(dx224Nterm)*/+, this value was 0.5% (n = 570). This also indicates that maternal *drp-1(+)* rescues the lethality of *drp-1(dx224Nterm)* and *drp-1(dx230Internal)* homozygotes.

Next, we examined the expression and subcellular localization of tagged DRP-1 protein in cleavage stage embryos. For this, we used TMRE (Tetramethylrhodamine ethyl ester) staining to assess colocalization between the mNG-tagged DRP-1 protein and mitochondria (Figure 1 B). Mitochondrial morphology and distribution during cleavage divisions were very similar between wild type N2 and *drp-1(dx230Internal)* embryos. By contrast, the morphology and distribution of mitochondria in *drp-1(dx224Nterm)* embryos were highly irregular; mitochondria were typically clustered in large aggregates and unequally distributed among blastomeres. This is consistent with a failure in mitochondrial fission. In the case of both *drp-1(dx230Internal)* and *drp-1(dx224Nterm)*, mNG signal was concentrated in foci that colocalized with mitochondria. Super-resolution imaging revealed that both proteins are closely associated with mitochondria (Figure 1 C). When the TMRE image is used to generate a mask of mitochondrial outlines, 95% of the mNG positive pixels are contained within the masked regions (see methods). DRP-1(dx230Internal) protein is present as discrete puncta ≤200 nm in diameter. These are likely to be ≤ 50 nm oligomeric assemblies of DRP-1 that constrict the mitochondria (Basu et al. 2017; Rosenbloom et al. 2014). Consistent with this idea, the mNG puncta typically coincide with regions of reduced TMRE fluorescence (Figure 1 D). DRP-1(dx224Nterm) protein tends to associate with mitochondria in the form of both puncta and filamentous aggregates; however, in this case mNG does not correlate with reduced TMRE signal (Figure 1 D). Finally, DRP-1(dx230Internal) protein appears to be present in a similar subcellular pattern in most if not all cells throughout embryogenesis and larval development as well as in adults.

Overall, our findings suggest that DRP-1 can function relatively normally in a biological context even when mNG is inserted into the variable domain. Therefore, it represents a powerful new tool for real time *in vivo* analyses.

Methods

Standard methods were used for *C. elegans* culture and genetic manipulations (Brenner 1974), except bacterial strain AMA1004 was used as a food source (Casadaban et al. 1983).

Wild type *C. elegans* N2 (Brenner 1974) was used as the starting strain for CRISPR modifications and for outcrossing edited strains. CRISPR editing was done essentially as described by Paix et al. (Paix et al. 2015), but ssDNA repair templates generated by asymmetric PCR were used on the recommendation of Eroglu et al. (Eroglu, Yu, and Derry 2023). F1 Dpy-10 animals with successful edits were identified by screening for mNG fluorescence using a Nikon SMZ18 epilfuorescence dissecting microscope. The edited *drp-1* alleles were then outcrossed from *dpy-10(lf)* using N2.

Reagents for CRISPR-Cas9 editing were obtained from IDT (Coralville, Iowa). Oligonucleotides for PCR were from Merck Life Science (UK). Q5 and LongAmp DNA polymerases were from NEB (UK).

Cas9 crRNA sequences were identified using CRISPOR (http://crispor.gi.ucsc.edu/crispor.py)(Concordet and Haeussler 2018).

Codon optimization and intron placement for mNG were determined using the *C. elegans* codon adapter (https://worm.mpi-cbg.de/codons/cgi-bin/optimize.py) (Redemann et al. 2011)

Imaging and image processing

Routine widefield imaging was done using a Zeiss AxioImager M2. Standard DIC optics were used and imaging was done using an EC Plan-Neofluar 100X/1.3 oil objective. For mNG imaging the same objective was used, but with a Colibri 7 LED light source 450-488 nm in combination with filter set 90. Images were acquired with a Photometrics Prime BSI sCMOS camera (USA) using ZEN Blue 2.6 software. For super resolution imaging, we used a Zeiss LSM 980 plus Airyscan 2 detector system. Imaging of mNG was done using 488 nm excitation and > 509 nm emission. Imaging of mScarlet I and TMRE were done separately from mNG using 552 nm excitation and > 578 nm emission. Acquisition parameters were adjusted in ZEN Blue 3.3 as necessary to optimize signal/noise ratio without excessive photobleaching. The standard autofilter setting was used for Airyscan processing.

Mitochondrial localization of DRP-1(dx230Internal) in Figure 1 C was quantified using Fiji as follows. The original pixel value range of the 16 bit images for mNG was 0-203, and for TMRE was 0-216. Images were thresholded by setting the pixel value range to 27-47, saving as 8 bit, then converting to binary mask. Next, Image math was used to subtract the TMRE values from the mNG image. Only 409/8011 filled pixels remained after subtraction, i.e., 94.9% of the signal was removed. When the same subtraction was performed with a TMRE image that was randomized after thresholding, 6662/8011 filled pixels remained, i.e., only 16.7% of the signal was removed.

TMRE staining was done by culturing worms overnight on NGM plates containing 100 nM TMRE (Molecular Probes, Thermo Fisher Scientific).

Reagents

Strain	Genotype	Notes		
N2	wild type var. Bristol	From CGC		
EJ1473	drp-1(dx230) mNG internal	This study		
EJ1480	drp-1(dx224) mNG N-terminal	This study		
DNA molecules	Sequence			
L766 mNeonF	cagtcaaattaaaacaat tttcagCAGCTACAACCGgg ttctggagccggggc	Use with L767 to amplify mNeonGreen from pEL336 to generate repair template for insertion into variable domain of drp-1.		
L767 mNeonR	GAAGAACAGCGTTCAAGT CGACACCATTAACTCCTGGC CCGCCAGATCCGGCTGA	See above		
Repair template for drp-1 internal	cagtcaaattaaaacaat tttcagCAGCTACAACCGgg ttctggagccggggcttcag	Repair template for internal insertion of mNeon. Homology		

	gcggtATGCCAGGATCTAAG GGAGAAGAGGATAACATGGC TT CCCTTCCAGCTACTCACG AACTTCATATTTTCGGATCT ATCAACGGAGTTGATTTCGA TATGGTTGGACAGgtaagtt taaacatatatatactaacta accctgattatttaaatt ttcagGGAACTGGAAATCCA AACGATGGATACGAAGAGCT TAACCTTAAGTCTACCAAGG GAGATCTTCAATTCTCTCC ATGGATCCTTGTCCCACA CATCGGATACGGATTCCACC AATACCTCCCATACCCAGAC GGAATGTCCCCATTCCAAGC TGCTATGGTTGATGGA TCTGGATACCAAGTTCAC CGCACTATGCAATTCGAGGA TGGAGCTTCCCTTACCGTTA ACTACCGCTACACTTACGAA GGATCTCACATCAAGG GAGAAGCTCAAGTTAAGG GAACTGGATTCCCAGCTGAT GGACCAGTTATGACCAACTC TCTTACCGCTGCTGATTGGT GCCGCTCTAAGgtaa cactatttttgtctctga accaactctttaaatttaaa tttcagAAGACTTACCCAAA CGATAAGACTATCATCTCTA CTTTCAAGTGGTCTTACACT ACTG GAAACGGAAAGCGCTACC GCTCTACCGCTCGCACTACC TACACCTTCGCTAAGCCAAT GGCCGCCAACTACCTCAAGA ACCAACCAATGTAC GTCTTCCGTAAGACCGAG CTCAAGCACTCCAAGACCGA GCTCAACTTCAAGGAGTGGC AAAAGGCCTTCACCGACGTC ATGGGAATGGACG AGCTCTACAAGGGATCAG GCgccggtgcttcagccgga tctggcgggCCAGGAGTTAA TGGTGTCGACTTGAACGCTG TTCTTC	arms in bold, introns lower case.		

L660 mNeonR	ATCCTGCCTAACGTTGCG AAAACATCtTGgAGcTTgTT aACaACgGGAATGAGATTTT CCATcccgccagatccggctga	Use with L722 to generate repair template for insertion of mNeonGreen at 5' end of drp-1.		
L722 mNeon F	atgatactctcatttcgattcaaaaattttaaatttta cagaATGCCAGGATCTAAGG GAGAAGAG	See above		
Repair template N terminal	atgatactctcatttcgattcaaaaattttaaatttta cagaATGCCAGGATCTAAGG GAGAAGAGGATAACATGGCT TCCCTTCCAGCTACTCACGA ACT TCATATTTTCGGATCTAT CAACGGAGTTGATTTCGATA TGGTTGGACAGgtaagttta aacatatatactaactaa ccctgattatttaaattttcagGGA ACTGGAAATCCAAACGAT GGATACGAAGAGCTTAACCT TAAGTCTACCAAGGGAGATC TTCAATTCTCTCCATGGATC CTTGTCCCACACATCG GATACGGATTCCACCAAT ACCTCCCATACCCAGACGGA ATGTCCCCATTCCAAGCTGC TATGGTTGATGGATCTGGAT ACCAAGTTCACCGCAC TATGCAATTCGAGGATGG AGCTTCCCTTACCGTTAACT ACCGCTACACTTACGAAGGA TCTCACATCAAGGGAGAAGC TCAAGTTAAGGGAAC TGGATTCCCAGCTGATGG ACCAGTTATGACCAACTCTC TTACCGCTGCTGATTGGTGC CGCTCTAAGgtaacactatt tttgtctctgaaccaactcttt aaatttaaatttcagAAG ACTTACCCAAACGATAAGAC TATCATCTCTACTTTCAAGT GGTCTTACACTACTGGAAAC GGAAAGCGCTACCGCTCT ACCGCTCGCACTACCTAC ACCTTCGCTAAGCCAATGGC CGCCAACTACCTCAAGAACC AACCAATGTACGTCTTCCGT AAGACCGAGCTCAAG	N-terminal repair template. Bolded sequences are flanking homology; synonymous changes introduced to prevent recleavage by Cas9 are indicated by lower case characters. The underlined "ag" sequence is the splice acceptor site for the SL1 trans-spliced leader. Non-bold sequences are mNeon, with introns indicated by lower case lettering.		

		CACTCCAAGACCGAGCTC AACTTCAAGGAGTGGCAAAA GGCCTTCACCGACGTCATGG GAATGGACGAGCTCTACAAG GGATCAGGCgccgg tgcttcagccggatctgg cgggATGGAAAATCTCATTC CcGTtGTtAAcAAGCTCCAA GATGTTTTCGCAACGTTAGG CAGGAT			
	pEL336	aaataccgcacagatgcg taaggagaaaataccgcatc aggcggccttaagggcctcg tgatacgcctatttttatag gttaatgtcatgataataatggtttcttagacg tcaggtggcacttttcgg ggaaatgtgcgcggaacccc tatttgtttatttttctaaa tacattcaaatatgtatccg ctcatgagacaataaccctg ataaatgcttcaata atattgaaaaaggaagag tatgagtattcaacatttcc gtgtcgcccttattcccttt tttgcggcattttgccttcc tgtttttgctcacccagaaa cgctggtgaaagtaaa agatgctgaagatcagtt gggtgcacgagtgggttaca tcgaactggatctcaacagc ggtaagatccttgagagttt tcgccccgaagaacgttttccaatgatgagca cttttaaagttctgctat gtggcgcggtattatcccgt attgacgccgggcaagagca actcggtcgccgcatacact attctcagaatgacttggttgagtactcaccagt cacagaaaagcatcttac ggatggcatgacagtaagag aattatgcagtgctgccata accatgagtgataacactgc ggccaacttacttctgacaacgatcggagga ccgaaggagctaaccgct tttttgcacaacatgggggga tcatgtaactcgccttgatc gttgggaaccggagctgaat gaagccataccaaacgacgagcgtgacacca cgatgcctgtagcaatgg caacaacgttgcgcaaacta ttaactggcgaactacttac	Phsp-16::mNeonGreen plasmid used as template for amplification of mNeon Green		

tctagcttcccggcaacaat
taatagactggatggaggcggataaagttgc

aggaccacttctgcgctc
ggcccttccggctggctggt
ttattgctgataaatctgga
gccggtgagcgtgggtctcg
cggtatcattgcagcactggggccagatggtaa

gccctcccgtatcgtagt
tatctacacgacggggagtc
aggcaactatggatgaacga
aatagacagatcgctgagat
aggtgcctcactgattaagcattggtaactgt

cagaccaagtttactcat
atatactttagattgattta
aaacttcatttttaatttaa
aaggatctaggtgaagatcc
tttttgataatctcatgaccaaaatcccttaacgt

gagttttcgttccactga
gcgtcagaccccgtagaaaa
gatcaaaggatcttcttgag
atccttttttctgcgcgta
atctgctgcttgcaaacaaa
aaaaccaccgctac

cagcggtggtttgtttgc
cggatcaagagctaccaact
ctttttccgaaggtaactgg
cttcagcagagcgcagatac
caaatactgtccttctagtgtagccgtagttagg

ccaccacttcaagaactc
tgtagcaccgcctacatacc
tcgctctgctaatcctgtta
ccagtggctgctgccagtgg
cgataagtcgtgtcttaccgggttggactcaaga

cgatagttaccggataag
gcgcagcggtcgggctgaac
ggggggttcgtgcacacagc
ccagcttggagcgaacgacc
tacaccgaactgagatacctacagcgtgag

cattgagaaagcgccacg
cttcccgaagggagaaaggc
ggacaggtatccggtaagcg
gcagggtcggaacaggagag
cgcacgagggagcttccagggggaaac

gcctggtatctttatagt
cctgtcgggtttcgccacct
ctgacttgagcgtcgatttt
tgtgatgctcgtcaggggggg
cggagcctatggaaaaacgc
cagcaacgcggcctt

tttacggttcctggcctt
ttgctggccttttgctcaca

tgttctttcctgcgttatcc
cctgattctgtggataaccg
tattaccgcctttgagtgag
ctgataccgctcgccgcag

ccgaacgaccgagcgcag
cgagtcagtgagcgaggaag
cggaagagcgcccaatacgc
aaaccgcctctccccgcgcg
ttggccgattcattaatgcagctggcacga

caggtttcccgactggaa
agcgggcagtgagcgcaacg
caattaatgtgagttagctc
actcattaggcaccccaggc
tttacactttatgcttccggctcgtatgttgtgt

ggaattgtgagcggataa
caatttcacacaggaaacag
ctatgaccatgattacgcca
agctgtaagtttaaacatga
tcttactaactaactattctcatttaaattttc

agagcttaaaaatggctg
aaatcactcacaacgatgga
tacgctaacaacttggaaat
gaaataagcttgcatgcctg
caggtcgactctagaggatcaccaaaaacg

gaacgttgagctggacgg
aaatagtggtaaagtgacat
gattatagtttgaagatttc
taatttcacaattagagcaa
atgttgttcggtatttattttcaacggtatttata

ctattttccacctttttc
tagaacattcgagctgcttg
ttgcaaaaggagggcgactc
acattcggtacatggaaaag
tagtgtacacaataaagagacccagatacattt

tccgtctgcgtctctttg
cacccaccgggagtattttc
aaacgaatgcatctaggacc
ttctagaacattctgtaagg
ctgcagaatgcgggtatata
aggaaagcgggct

cagaggaagccaacacgc
tttgttctagtgcatctaaa
aaacttcgaaaatcctcatc
gggatcctatcgattcgcgg
ccgctgtacacccccaaaggacccaaaggtat

gtttcgaatgatactaac
ataacatagaacattttcag
gaggacccttggagggtacc
gagctcagaaaaaactagtt
AtgGGTTCCTGTATTGGAAa
AATGgCTc

ccggttctggagccgggg
cttcaggcggtATGCCAGGA
TCTAAGGGAGAAGAGGATAA
CATGGCTTCCCTTCCAGCTA
CTCACGAACTTCATATTTTC

GGATCTATCAACGGAGTT
GATTTCGATATGGTTGGACA
Ggtaagtttaaacatatata
tactaactaaccctgattat
ttaaattttcagGGAACTGGAAAT

CCAAACGATGGATACGAA
GAGCTTAACCTTAAGTCTAC
CAAGGGAGATCTTCAATTCT
CTCCATGGATCCTTGTCCCA
CACATCGGATACGGAT

TCCACCAATACCTCCCAT
ACCCAGACGGAATGTCCCCA
TTCCAAGCTGCTATGGTTGA
TGGATCTGGATACCAAGTTC
ACCGCACTATGCAATT

CGAGGATGGAGCTTCCCT
TACCGTTAACTACCGCTACA
CTTACGAAGGATCTCACATC
AAGGGAGAAGCTCAAGTTAA
GGGAACTGGATTCC

CAGCTGATGGACCAGTTA
TGACCAACTCTCTTACCGCT
GCTGATTGGTGCCGCTCTAA
Ggtaacactatttttgtctc
tgaaccaactctttaaatttaaat

ttcagAAGACTTACCCAA
ACGATAAGACTATCATCTCT
ACTTTCAAGTGGTCTTACAC
TACTGGAAACGGAAAGCGCT
ACCGCTCTACCGCTCGC

ACTACCTACACCTTCGCT
AAGCCAATGGCCGCCAACTA
CCTCAAGAACCAACCAATGT
ACGTCTTCCGTAAGACCGAG
CTCAAGCACTCCAAG

ACCGAGCTCAACTTCAAG
GAGTGGCAAAAGGCCTTCAC
CGACGTCATGGGAATGGACG
AGCTCTACAAGGGATCAGGC
gccggtgcttcagccg

gatctggcgggCtgatcg
acgccaacgtcgttgaattt
tcaaattttaaatactgaat
atttgtttttttcctattatttatttattctctttgtgt
ttttttcttgctttctaaaa

	aattaattcaatccaaatctaaacatttttttttctct ttccgtctcccaattcgtat tccgctcctctcatctgaac acaatgtgcaagtttattta tcttctcgctttcatttcat taggacgtgggggggaatt ggtggaaggggggaaacacac aaaaggatgatggaaatgaa ataaggacacacaatatgca acaacattcaattcagaaatatggagg aaggtttaaaagaaaaca taaaaatatatagaggagga aggaaaactagtaaaaaata agcaaagaaattaggcgaac gatgagaattgtcctcgcttgggccctt tcgtctcgcgcgtttcgg tgatgacggtgaaaacctct gacacatgcagctcccggag acggtcacagcttgtctgta agcggatgccgggagcagac aagcccgtcagg gcgcgtcagcgggtgttg gcgggtgtcggggctggctt aactatgcggcatcagagca gattgtactgagagtgcaccatatgcggtgtg			
Cas9 guide RNAs	Sequence			
DRP1.1	ACACCAUUAACUCCUGGUAC	crRNA for internal insertion of mNeon		
DRP1.2	UCCUGUAGUUUAUUGACG AC	crRNA for N-terminal tagging		
DPY-10	GCUACCAUAGGCACCACGAG	No repair template was used		
Fusion protein junctional sequence	Amino acid sequence			

mNeon::DRP-1 (N-terminal mNeon)	MPGSKGEEDNMASLPATH ELHIFGSINGVDFDMVGQGT GNPNDGYEELNLKSTKGDLQ FSPWILVPHIGYGFHQYLPY PDGMSPFQAAM VDGSGYQVHRTMQFEDGA SLTVNYRYTYEGSHIKGEAQ VKGTGFPADGPVMTNSLTAA DWCRSKKTYPNDKTIISTFK WSYTTGNGKRYR STARTTYTFAKPMAANYL KNQPMYVFRKTELKHSKTEL NFKEWQKAFTDVMGMDELYK GSGAGASAGSGGMENLIP	Underlined sequence is flexible linker. Bold is beginning of DRP-1.		
		DRP-1::mNeon::DRP-1 (internal mNeon)	VSAHGEQQLQPGSGAGAS GGMPGSKGEEDNMASLPATH ELHIFGSINGVDFDMVGQGT GNPNDGYEELNLKSTKGDLQ FSPWILVPHIGYGFHQYLPY PDGMSPFQAAMVDGSGYQVH RTMQFEDGASLTVNYRYTYE GSHIKGEAQVKGTGFPADGP VMTNSLTAADWCRSKKTYPN DKTIISTFKWSYTTGNGKRY RSTARTTYTFAKPMAANYLK NQPMYVFRKTELKHSKTELN FKEWQKAFTDVMGMDELYKG SGAGASAGSGGPGVNG	DRP-1 flanking residues in bold. Underlined residues are flexible linker sequences. A single valine was deleted from DRP-1 at the junction.

Acknowledgements: We thank Ms. Louisa McGuinness for excellent technical assistance.

References

Labrousse AM, Zappaterra MD, Rube DA, Van Der Bliek AM. 1999. C. elegans dynamin-related protein DRP-1 controls severing of the. Mol. Cell. 4: 815-826. DOI: 10.1016/s1097-2765(00)80391-3

Smirnova E, Griparic L, Shurland DL, Van Der Bliek AM. 2001. Dynamin-related protein Drp1 is required for mitochondrial division in. Mol. Biol. Cell. 12: 2245-2256. DOI: 10.1091/mbc.12.8.2245

Bleazard W, Mc Caffery JM, King EJ, Bale S, Mozdy A, Tieu Q, Nunnari J, Shaw JM. 1999. The dynamin-related GTPase Dnm1 regulates mitochondrial fission in yeast. Nat. Cell Biol. 1: 298-304. DOI: 10.1038/13014

Tabara LC, Segawa M, Prudent J. 2025. Molecular mechanisms of mitochondrial dynamics. Nat. Rev. Mol. Cell Biol. 26: 123-146. DOI: 10.1038/s41580-024-00785-1

Kamerkar SC, Liu A, Higgs HN. 2025. Mitochondrial fission - changing perspectives for future progress. J. Cell Sci. 138 DOI: 10.1242/jcs.263640

Kalia R, Wang RYR, Yusuf A, Thomas PV, Agard DA, Shaw JM, Frost A. 2018. Structural basis of mitochondrial receptor binding and constriction by. Nature. 558: 401-405. DOI: 10.1038/s41586-018-0211-2

Rochon K, Bauer BL, Roethler NA, Buckley Y, Su CC, Huang W, et al., Mears JA. 2024. Structural basis for regulated assembly of the mitochondrial fission. Nat. Commun. 15: 1328. DOI: 10.1038/s41467-024-45524-4

Roy K, Pucadyil TJ. 2022. Is Drp1 sufficient to catalyze membrane fission?. Proc. Natl. Acad. Sci. U. S. A. 119: e2201709119. DOI: 10.1073/pnas.2201709119

Perez Jover I, Madan Mohan P, Ramachandran R, Shnyrova AV. 2022. Reply to Roy and Pucadyil: A gain of function by a GTPase-impaired Drp1. Proc. Natl. Acad. Sci. U. S. A. 119: e2202391119. DOI: 10.1073/pnas.2202391119

Montecinos Franjola F, Bauer BL, Mears JA, Ramachandran R. 2020. GFP fluorescence tagging alters dynamin-related protein 1 oligomerization. Sci. Rep. 10: 14777. DOI: 10.1038/s41598-020-71655-x

Strack S, Cribbs JT. 2012. Allosteric modulation of Drp1 mechanoenzyme assembly and mitochondrial. J. Biol. Chem. 287: 10990-11001. DOI: 10.1074/jbc.M112.342105

Liu R, Chan DC. 2015. The mitochondrial fission receptor Mff selectively recruits oligomerized. Mol. Biol. Cell. 26: 4466-4477. DOI: 10.1091/mbc.E15-08-0591

Bui HT, Karren MA, Bhar D, Shaw JM. 2012. A novel motif in the yeast mitochondrial dynamin Dnm1 is essential for. J. Cell Biol. 199: 613-622. DOI: 10.1083/jcb.201207079

Mahajan M, Bharambe N, Shang Y, Lu B, Mandal A, Madan Mohan P, et al., Ramachandran R. 2021. NMR identification of a conserved Drp1 cardiolipin-binding motif essential. Proc. Natl. Acad. Sci. U. S. A. 118: e2023079118. DOI: 10.1073/pnas.2023079118

Sternberg PW, Van Auken K, Wang Q, Wright A, Yook K, Zarowiecki M, et al., Stein L. 2024. WormBase 2024: status and transitioning to Alliance infrastructure. Genetics. 227 DOI: 10.1093/genetics/iyae050

Kamerkar SC, Kraus F, Sharpe AJ, Pucadyil TJ, Ryan MT. 2018. Dynamin-related protein 1 has membrane constricting and severing abilities. Nat. Commun. 9: 5239. DOI: 10.1038/s41467-018-07543-w

Basu K, Lajoie D, Aumentado Armstrong T, Chen J, Koning RI, Bossy B, et al., Rouiller I. 2017. Molecular mechanism of DRP1 assembly studied in vitro by cryo-electron. PLoS One. 12: e0179397. DOI: 10.1371/journal.pone.0179397

Rosenbloom AB, Lee SH, To M, Lee A, Shin JY, Bustamante C. 2014. Optimized two-color super resolution imaging of Drp1 during mitochondrial. Proc. Natl. Acad. Sci. U. S. A. 111: 13093-13098. DOI: 10.1073/pnas.1320044111

Brenner S. 1974. The genetics of Caenorhabditis elegans. Genetics. 77: 71-94. DOI: 10.1093/genetics/77.1.71

Casadaban MJ, Martinez Arias A, Shapira SK, Chou J. 1983. Beta-galactosidase gene fusions for analyzing gene expression in. Methods Enzymol. 100: 293-308. DOI: 10.1016/0076-6879(83)00063-4

Paix A, Folkmann A, Rasoloson D, Seydoux G. 2015. High efficiency, homology-directed genome editing in Caenorhabditis. Genetics. 201: 47-54. DOI: 10.1534/genetics.115.179382

Eroglu M, Yu B, Derry WB. 2023. Efficient CRISPR/Cas9 mediated large insertions using long single-stranded. FEBS J DOI: 10.1111/febs.16876

Concordet JP, Haeussler M. 2018. CRISPOR: intuitive guide selection for CRISPR/Cas9 genome editing. Nucleic Acids Res. 46: W242-W245. DOI: 10.1093/nar/gky354

Redemann S, Schloissnig S, Ernst S, Pozniakowsky A, Ayloo S, Hyman AA, Bringmann H. 2011. Codon adaptation-based control of protein expression in C. elegans. Nat. Methods. 8: 250-252. DOI: 10.1038/nmeth.1565

Funding: This work was funded by a Wolfson Fellowship from the Royal Society (RSWF\R1\180008) and BBSRC Responsive Mode Grants (BB/V007572/1 and BB/V015648/1) to B.C.

Author Contributions: Eric J. Lambie: conceptualization, formal analysis, investigation, methodology, validation, visualization, writing - original draft. Barbara Conradt: conceptualization, funding acquisition, project administration, resources, writing - review editing.

Reviewed By: Anonymous

Nomenclature Validated By: Anonymous

WormBase Paper ID: WBPaper00068111

History: Received March 29, 2025 **Revision Received** April 22, 2025 **Accepted** May 6, 2025 **Published Online** May 8, 2025 **Indexed** May 22, 2025

5/8/2025 - *Open Access*

Citation: Lambie EJ, Conradt B. 2025. Insertion of mNeonGreen into the variable domain of DRP-1 permits visualization of functional endogenous protein. microPublication Biology. 10.17912/micropub.biology.001588